Available online at www.sciencedirect.com

SciVerse ScienceDirect

journal homepage: www.elsevier.com/locate/he

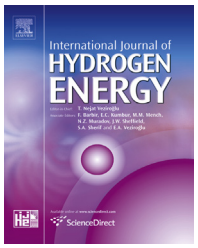

Sulfonated graphene oxide/Nafion composite membranes for high-performance direct methanol fuel cells

Hung-Chung Chien [b,c], *Li-Duan Tsai* [c], *Chiu-Ping Huang* [b], *Chi-yun Kang* [b], *Jiunn-Nan Lin* [b], *Feng-Chih Chang* [a,c,d,*]

[a] *Department of Materials and Optoelectronic Science, Center for Nanoscience and Nanotechnology, National Sun Yat-Sen University, Kaohsiung 804, Taiwan*

[b] *Material and Chemical Research Laboratories, Industrial Technology Research Institute, Chutung, Hsinchu 310, Taiwan*

[c] *Department of Applied Chemistry, National Chiao Tung University, Hsinchu 300, Taiwan*

[d] *R&D Center for Membrane Technology, Chung Yuan Christian University, Chungli, Taoyuan, Taiwan*

ARTICLE INFO

Article history:
Received 18 March 2013
Received in revised form
2 August 2013
Accepted 6 August 2013
Available online 5 September 2013

Keywords:
Nafion
Sulfonated graphene oxide
Methanol crossover
Direct methanol fuel cells

ABSTRACT

An easy and effective method for producing low methanol-crossover membranes is developed by dispersing sulfonated graphene oxide (SGO) into a Nafion matrix. A SGO/Nafion mixture with low SGO content exhibits unique viscosity behavior and allows for better SGO dispersion within the Nafion. After film casting, the composite membranes show lower methanol and water uptakes, a reduced swelling ratio, improved proton conductivity in low relative humidity, and extremely high methanol selectivity, which can be implemented in direct methanol fuel cells (DMFCs). The regular backbone of the composite membrane shows a higher storage modulus, increased α-relaxation (transition temperature), and improved tolerance to pressure during membrane electrode assembly (MEA). The small angle X-ray spectra indicate the shrinkage of the ionic clusters in the composite membranes, which thus reduce methanol crossover. The hybrid membranes applied to DMFCs demonstrate performances superior to that of the commercial Nafion 115 in 1 M and 5 M methanol solutions.

1. Introduction

Direct methanol fuel cells (DMFCs) have attracted considerable attention from those interested in alternative fuels and merit further investigation. These alternative energy devices can be applied to power a wide range of portable and mobile electronics because DMFCs employ easily manageable liquid methanol fuel with excellent energy storage densities. DMFCs provide uninterrupted, continuous power as long as the methanol fuel is supplied because they are energy conversion devices rather than energy storage devices. Moreover, DMFCs provide higher energy densities than Li-ion batteries. DMFCs consist of an anode, a cathode, and a proton-conducting electrolyte membrane, which collectively are called a

* *Corresponding author*. R&D Center for Membrane Technology, Chung Yuan Christian University, Chungli, Taoyuan, Taiwan. Tel./fax: +886 3 5131512.
E-mail addresses: changfc1973@gmail.com, changfc@mail.nctu.edu.tw (F.-C. Chang).

0360-3199/$ – see front matter
http://dx.doi.org/10.1016/j.ijhydene.2013.08.036

membrane electrode assembly (MEA). The current DMFC research is based on polymer electrolyte membranes that provide appropriate fuel cell performance in terms of conductivity, chemical and mechanical stability, durability, and fuel crossover [1–3].

Among the polymer electrolyte membranes, DuPont's perfluorosulfonic acid polyelectrolyte, Nafion, is commonly used because of its excellent chemical stability and high proton conductivity. However, Nafion has a high methanol permeability, referred to as methanol crossover, attributed to the transport of methanol together with water molecules through its ion cluster channels. Moreover, the permeation of methanol from the anode to the cathode is a major challenge for the practical commercialization of DMFCs, due to the degraded cell performance of the mixed potential and catalyst poisoning problems [4,5]. To reduce methanol crossover, thicker membranes such as Nafion 117 (175 μm in thickness) are often preferred for DMFCs. However, this approach causes an increase in resistance and a decrease in power density [6].

To address the methanol crossover problems, many research groups have focused on the modification of Nafion membranes with a variety of nanofillers and polymers, such as SiO_2, zeolites, zirconium, and polypyrrole [7–13]. The reported strategies for improving the performance of Nafion can be divided into two approaches: either incorporation of dispersed nanofillers [14] or formation of the nanocomposite membranes by in situ formation of inorganic fillers [15]. The composite membranes show high water uptake and low methanol crossover, compared to neat Nafion. However, the organic–inorganic membranes prepared by the above mentioned methods become brittle and poorly conductive, due to the high loading of the inorganic materials. Here, we report a novel strategy for producing low methanol-crossover polymer electrolytes using sulfonated graphene oxide (SGO) [16].

Currently, GO is highly attractive for many applications as a result of its outstanding thermal and mechanical properties [17,18]. Graphene oxide sheets can be thought as an amphiphilic material with hydrophilic regions that contain hydroxyl, carboxylic, and epoxy groups, and hydrophobic regions composed of sp^2 graphite. GO has been used as a surfactant to disperse C_{60} and acts as a hole transporting layer for all-carbon solar cells [19]. Moreover, GO/conducting polymer composites have shown superior capacitance and long cycle life in supercapacitors [20]. The potential advantages of using GO to improve the performance of DMFCs have not been fully realized. Choi group showed outstanding DMFC performance by introducing GO into Nafion solution [21]. However, the image of the GO/Nafion composite membrane revealed inhomogeneous distribution of the GO. Surfactant adsorbed GO has also been investigated on the sulfonated poly(ether ether ketone) (SPEEK) and shown improved proton conductivity and reduced methanol permeability [22]. One of the challenges is to avoid the aggregation of the GO in the polymer matrix. To address this matter, we determined the viscosity changes of the sulfonated GO (SGO)/Nafion solution. The optimal loading percentage of the SGO to Nafion was less than 1.0 wt%. Our investigation revealed a structural reorganization in the composite, showing clearly that the incorporation of the proper amount of SGO in Nafion enhanced proton conductivity, reduced the water and methanol uptakes, decreased methanol permeability, and improved the mechanical properties.

2. Experimental section

2.1. Materials

Nafion 212 and 18% Nafion DE2020 dispersion were obtained from Ion Power Inc., New Castle, Delaware, U.S. PtRu/C and Pt/C were purchased from Johnson Matthey Inc., and used without further purification. Sulfuric acids (H_2SO_4, Scharlau, 95–98%) was used without further purification.

2.2. Preparation of sulfonated graphene oxide (SGO)

Graphite oxide was prepared from flake graphite powder by a modified Hummers method [23]. In brief, graphite oxide was synthesized by an oxidation of graphite with $KMnO_4$ and $NaNO_3$ in concentrated sulfuric acid. The oxidation was carried out using 250 ml of concentrated sulfuric acid per 10 g of graphite as the dispersion medium. To the graphite dispersion, 5 g $NaNO_3$ were added and cooled the dispersion to 0 °C by using the ice water bath. Then 30 g of $KMnO_4$ were added slowly during 5 h. When the addition was finished, the resulting mixture was stirred at room temperature for another 5 h. The reaction was quenched by pouring ice cold water and adding 5% H_2O_2 to destroy unreacted $KMnO_4$. The graphite oxide was collected and washed with $HCl_{(aq)}$ and DI water. The brown graphite oxide was dried under the vacuum. To prepare graphene oxide (GO), 100 mg graphite oxide was dispersed in 100 ml of DI and ultrasonicated with power 100 W (misonix, sonicator 3000) for hours until the solution became clear. Then the GO solution was centrifuged with 4000 rpm for 10 min to remove any unexfoliated graphite oxide.

50 mg graphene oxide was added to 8 ml 0.06 M sulfanilic acid solution at 70 °C. Under continuous stirring, 2 ml 6×10^{-3} M sodium nitrite solution was added dropwise and the mixture held at 70 °C for 12 h. After the reaction, the mixture was washed collected by centrifuge and washed with water for several times until the pH reached 7. The SGO particles were characterized by XPS (X-ray photoelectron spectroscopy, Thermo VGESCAlab 250).

2.3. Manufacture of proton exchange membranes

Nafion ionomers were transferred to N,N-dimethylacetamide (DMAc, Aldrich) by distilling a mixed solution of the Nafion DE2020 solution (500 ml, 18% dispersion in aqueous alcohol) and DMAc (500 ml) under reduced pressure until the solution temperature reached 70 °C, to remove water and solvent. SGO/Nafion solutions with different SGO loadings in DMAc were prepared by adding well-dispersed $SGO_{(aq)}$ into the Nafion solution and mixing by mild ultrasonication for 6 h. Then, the SGO/Nafion solutions were degassed and dispersed with a planetary mixer before casting. The composite membranes were obtained from bar coating and drying at 50 °C for 24 h, and post annealing at 140 °C for 2 h. Nafion composite membranes of the desired sizes were placed into 0.5 M $H_2SO_{4(aq)}$ at

80 °C for 1 h to activate the sulfonic acids of the Nafion. Then, the activated membranes were soaked at 80 °C in DI water to remove excess acid on the membrane.

2.4. Fabrication of membrane electrode assembly (MEA)

PtRu/C catalysts of nominal 1:1 atomic ratio and Pt catalysts, both supported on conductive carbon black, were obtained from Johnson Matthey, Inc. The mean particle sizes of the catalysts ranged between 2.5 and 4 nm. Anode inks were made by dispersing appropriate amounts of the supported PtRu/C catalyst, deionized water, and Nafion dispersion. The cathode inks contained supported Pt catalysts, deionized water, and Nafion dispersion. The catalyst inks were vigorously stirred until the mixtures became smooth pastes. The inks were coated onto gas diffusion layers; the loadings of the PtRu for the anode and the Pt for the cathode were 2 mg cm^{-2} each. Membrane electrode assemblies were hot pressed under a pressure of 25 kg cm^{-2} at 130 °C for 3 min.

2.5. Dynamic rheological measurement

Dynamic rheological measurements were measured by a strain-controlled rheometer (TA, ARES LS1) equipped with a plate–plate geometry (diameter 8.0 mm, gap 0.5 mm). Angular frequency sweeps were carried out in the range from 10^{-1} to 10^{2} rad s^{-1} at 30 °C.

2.6. Proton conductivity

The impedance spectra of the membranes at various humidity levels were measured by a four-point probe unit in a temperature and humidity test chamber (MHK, Terchy Environmental Technology, Ltd.) using a Bio-Logic SP-300 Analyser within the range 7 MHz–0.1 Hz with a voltage amplitude of 0.01 V. The resistance of the membranes was calculated from the intercept of the real axis in the intermediate frequency domain of the impedance spectrum (Z″ vs. Z′). The measurements were conducted at 30 °C and the membranes were equilibrated for 1 h at different relative humidity (RH) levels. Ultimately, the proton conductivity σ was calculated based on the equation:

$$\sigma = L/AR \tag{1}$$

where L is the sample thickness, A is the cross-sectional area, and R is the resistance of the membrane.

2.7. Water and methanol uptake, and swelling ratio

The liquid-equilibrated water (and methanol) uptakes of the membranes were calculated from the equation:

$$WU = (W_{wet}\text{-}W_{dry})/W_{dry} \tag{2}$$

where W_{wet} and W_{dry} are the weights of the fully hydrated and the anhydrous membranes, respectively. The membranes were first immersed in deionized water (or methanol at 30 °C) for 24 h, blotted with an absorbent paper, and then, W_{wet} was measured. Subsequently, the membranes were thoroughly dried in a vacuum oven at 70 °C for 24 h; then, W_{dry} was measured. The dimensions of the hydrated and dry membranes were measured with a micrometer (Mitutoyo) that was able to measure the membrane thickness with micrometer resolution [24].

The swelling ratio (Sr) was obtained using the wet and the dry lengths of the membrane, designated as L_{wet} and L_{dry}, respectively. The Sr can be calculated by following equation:

$$Sr = (L_{wet}\text{-}L_{dry})/L_{dry} \times 100(\%) \tag{3}$$

2.8. Ion exchange capacity, methanol permeability and mechanical properties

Ion exchange capacity (IEC) was measured by soaking the membrane into 50 ml 1 M $NaCl_{(aq)}$ for 12 h. Then, the membrane was taken out and titrated the $NaCl_{(aq)}$ with 0.01 M $NaOH_{(aq)}$ until the pH value reached 7 (pH meter, Suntex SP-2200).

The methanol permeability of the membrane was determined using a two-chamber liquid permeability cell with 20 v/v% $MeOH_{(aq)}$. The methanol permeability is based on methanol crossover the membrane for the concentration difference. The methanol permeability is calculated according to the following equation:

$$C_B(t) = (A/V_B)D(K/L)C_A(t\text{-}t_0) \tag{4}$$

where C is concentration, V_B is the volume of the solution in the methanol permeation side, A and L are the membrane area and thickness respectively; D and K, are respectively, the methanol diffusivity and partition coefficient. Assume that D inside the membrane is constant and K is independent to the concentration. The product DK is the membrane permeability. t_0, referred as the time lag, is related to the diffusivity as $t_0 = L^2/6D$. C_B has been monitored by density meter (Auton Paar, DMA 4500). The methanol permeability was calculated from the slope of the straight line plot straight line plot obtained between $C_B(t)$ against time. [25]

Dynamic mechanical analyses (DMAs) of the rectangular films were carried out on a TA Instruments Q800 using a film/fibre tension clamp within the temperature range 35 °C–150 °C (scanning rate: 3 °C per min; applied strain: 0.3%; single frequency: 10 Hz).

2.9. Wide angle X-ray scattering (WAXS) and small angle X-ray scattering (SAXS)

Nafion and SGO/Nafion composite membranes were dried in a vacuum oven and stored in a plastic bag before the measurement. WAXS measurements were performed on a powder X-ray diffractometer (PANalytical, PW3040) to characterize the changes of the Nafion composite membranes. SAXS measurements were made on a Bruker Nanostar instrument under vacuum to determine the changes of the ionic clusters.

3. Results and discussion

3.1. Preparation of sulfonated graphene oxide

The sulfonation of the GO was confirmed by the XPS as shown in Fig. 1. After oxidation of the graphite by the modified

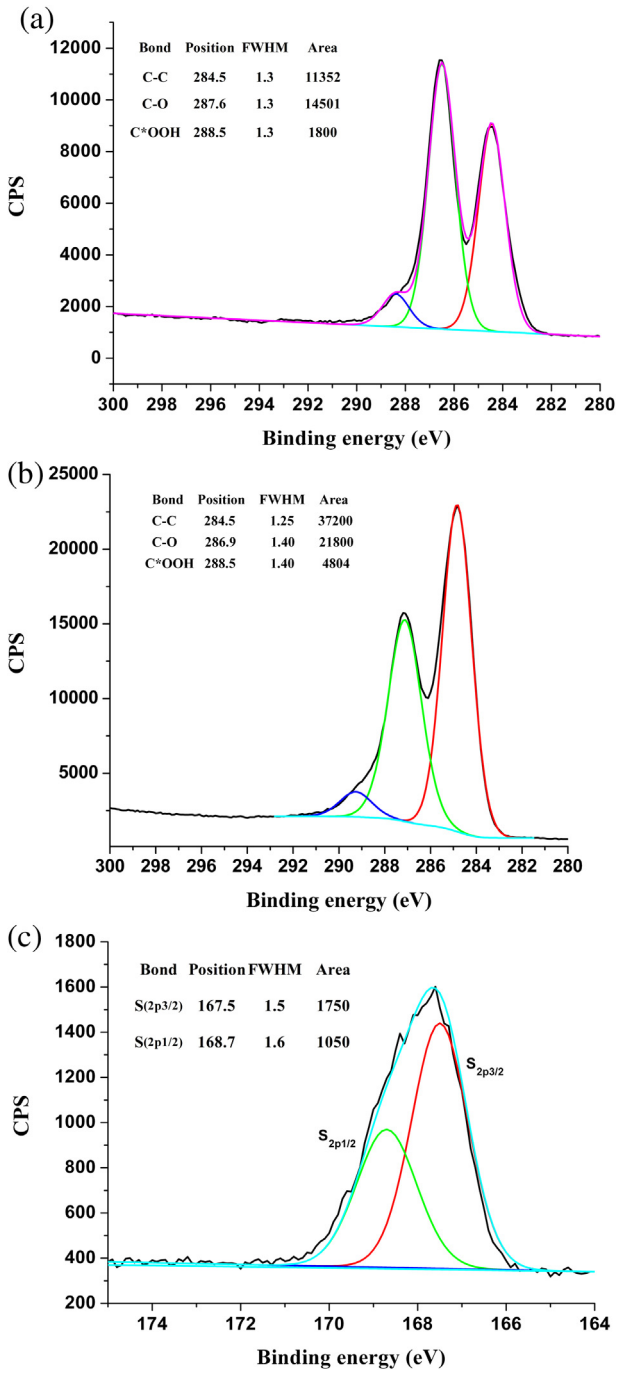

Fig. 1 – XPS C1s spectra of GO (a), SGO (b) and S2p spectra of SGO (c).

Hummers method, the characteristic peaks of GO were appeared at C–C (284.5 eV), C–O (287.6 eV), C=O (288.5 eV) in C1s spectrum. Compared to the GO, a new peak of S2p appeared at SGO due to the $-PhSO_3^-$ groups anchored on the GO backbones. Moreover, the ratio of the C–C/C–O changes from 0.78 to 1.70. The increase in C–C intensity was contributed the successful modification of the benzenesulfonyl group. The SGO was intrinsically non-electric conductive due to the abundant functionalized group on the surface.

To ensure the quality of the initial material, the exfoliated SGO were centrifuged at 4000 rpm to remove the larger and unexfoliated SGO. The well-exfoliated SGO was further characterized by SEM and TEM. As shown in Fig. 2(a), the wrinkled morphology without visible aggregation suggested the highly flexible characteristic of the SGO. Further, the cross-section image (Fig. 2(b)) and TEM image (Fig. 2(c)) revealed that the exfoliated SGO were easy to restack and formed layered structure.

3.2. *Rheological properties of the SGO/Nafion solution*

The pure Nafion solution was transparent, and the color of the SGO/Nafion mixture changed to brownish as the SGO loading increased. The viscosity of the Nafion solution dramatically changed after the incorporation of SGO (Fig. 3). At low SGO content, the viscosity was initially increased due to the interaction between the acid groups of SGO and Nafion. However, the viscosity was reduced slightly when the SGO loading percentage exceeded 0.5 wt%. The maximum viscosity (5 times higher than the pure Nafion solution) was achieved at 0.5 wt%, revealing that the SGO/Nafion solution was homogeneously dispersed. A previous literature report described the significant increase in viscosity of a mixture of graphene oxide and PEDOT/PSS [26]. The slight reduction in our observed viscosity can be explained by the limited dispersion behavior of SGO in the Nafion/DMAc matrix: agglomeration resulted in the reduced surface area between the SGO and Nafion, and caused the decrease in viscosity.

3.3. *Characterization of the composite membrane*

The SGO/Nafion composite membranes were obtained according to the described experimental steps. The appearance of the composite membrane changed from transparent to brownish, as shown in Fig. 4(a). The SEM image of the cross section of the 0.5 wt% composite membrane in Fig. 4(b) showed good SGO dispersion in the matrix without any obvious interface separation or voids. The TEM image (Fig. 4(c)) revealed that the SGO particles were well-oriented within the matrix and perpendicular to the pathway of the fuel. The fully exfoliated SGO sheets were dispersed homogeneously into the Nafion matrix for the hydrogen bonding between SGO and Nafion, and horizontally aligned to the substrate during the drying process.

Further, the drying process is an important step for high quality proton exchange membrane due to the phase separation may take place during the drying process and results in inhomogeneous membranes, which include pin holes and internal stresses. Fig. 5 shows the powder X-ray diffraction (PXRD) results for different loading percentages of the SGO/Nafion composite membranes. The SGO had an obvious diffraction peak at 10°, which was evidence of oxidized graphite. The broad peak at 17° was assigned to the crystallinity of the PTFE backbone in the pure Nafion membrane. As the SGO loading increased from 0.05 to 2 wt%, the intensity of the Nafion crystallized peak was reduced, which indicated a progressive decrease in the crystallinity of the Nafion matrix. Meanwhile, the characteristic peak of the SGO appeared at loadings higher than 0.5 wt%, and its intensity increased with

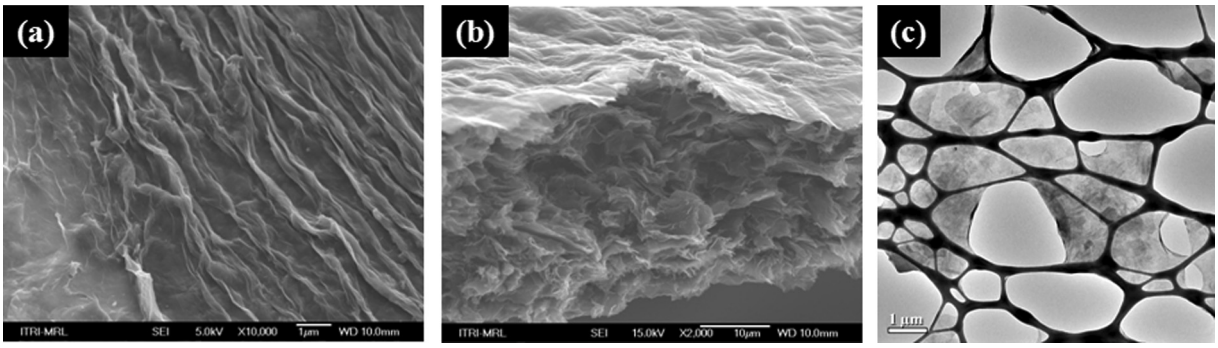

Fig. 2 – SEM image and TEM image of the SGO.

increasing SGO loading. This revealed unexfoliated SGO and the limited dispersion behavior of SGO in a Nafion matrix. The optimal ratio for the SGO/Nafion composite membrane was in the range of 0.05 and 0.5 wt%, which corresponded well with the rheological results.

3.4. *Water and methanol uptakes, and the swelling ratio of the composite membrane*

3.4.1. *Water and methanol uptakes*

Table 1 shows the water and methanol uptakes of the composite membranes. The water uptake was slightly reduced to 24% as the SGO loading reached 0.5 wt%, which was nearly 6% lower than the recast Nafion membrane. Protons are transported through the membrane with the water molecules, and generally accompany methanol during the operation of the DMFCs. The reduced water uptake indicated a shrinkage of the ionic channels, which impedes the transport of water and methanol. However, as the loading exceeded 0.5 wt%, the water uptake increased slightly due to SGO aggregation. Methanol uptake was tested at two different concentrations. The recast Nafion showed high methanol uptake, implying that Nafion is methanol favorable. In contrast, the SGO/Nafion composite membranes had lower methanol uptakes at both concentrations of methanol. Furthermore, the methanol uptake ratio followed the trend of the water uptake, which revealed that the formation of a physical cross-linking network with SGO junctions had enhanced connection between ionic clusters [27].

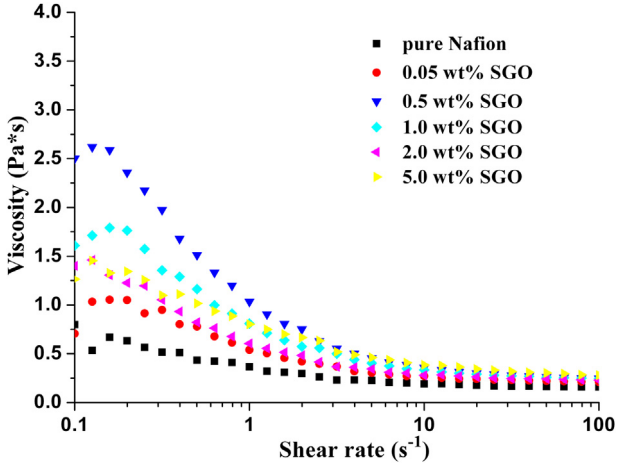

Fig. 3 – Rheological spectra of pure Nafion solution and different SGO loadings of SGO/Nafion solutions.

3.4.2. *Swelling ratio*

The structural features of Nafion, derived from the hydrophilic sulfonic acid side groups and the nonpolar fluorocarbon backbone, result in phase separation. Based on small angle X-ray scattering (SAXS) studies, Gierke proposed that the sulfonic acid groups were clustered in spherical domains [28]. The water-swollen ionic domains were treated as inverse micelles—essentially, pools of water—and it was proposed that water and ion transport occurred through narrow interconnecting channels [29]. The swelling ratio was strongly related to the solvent uptake. The swelling ratios of the SGO/Nafion composite membranes were determined for two different methanol solution concentrations, as shown in Table 2. The Nafion membrane showed a high swelling ratio in methanol solution because of the high swelling of the ionic clusters. Expansion in the ionic channels allows methanol to pass through the membrane much more easily. In contrast, the 0.5 wt% SGO/Nafion composite membrane exhibited swelling ratios of 14.5 and 32.2% in 20 and 50% (v/v) methanol solutions, respectively. The results of the swelling ratios were consistent with the methanol uptake results, which revealed that the highly stable composite membranes had good methanol-blocking properties and met the requirement for methanol stability in fuel cells for portable applications.

3.5. *Small angle X-ray scattering*

The SAXS spectrum of Nafion exhibited the following scattering features: (i) a matrix knee at a scatter vector (q) value of around 0.6 nm^{-1}, attributed to the semi-crystalline nature of the perfluorosulfonic acid backbone; (ii) an ionomer scattering peak at a q value which was dependent on the water content of the membrane; and (iii) in the Porod regime, a strong reduction of the scattering intensity that suggested the existence of an interface between the polymer and water [30,31]. The ionomeric peak has been extensively studied, but remains subject to controversy. Several models have been adopted to describe the morphology of cluster domains (i.e. spherical,

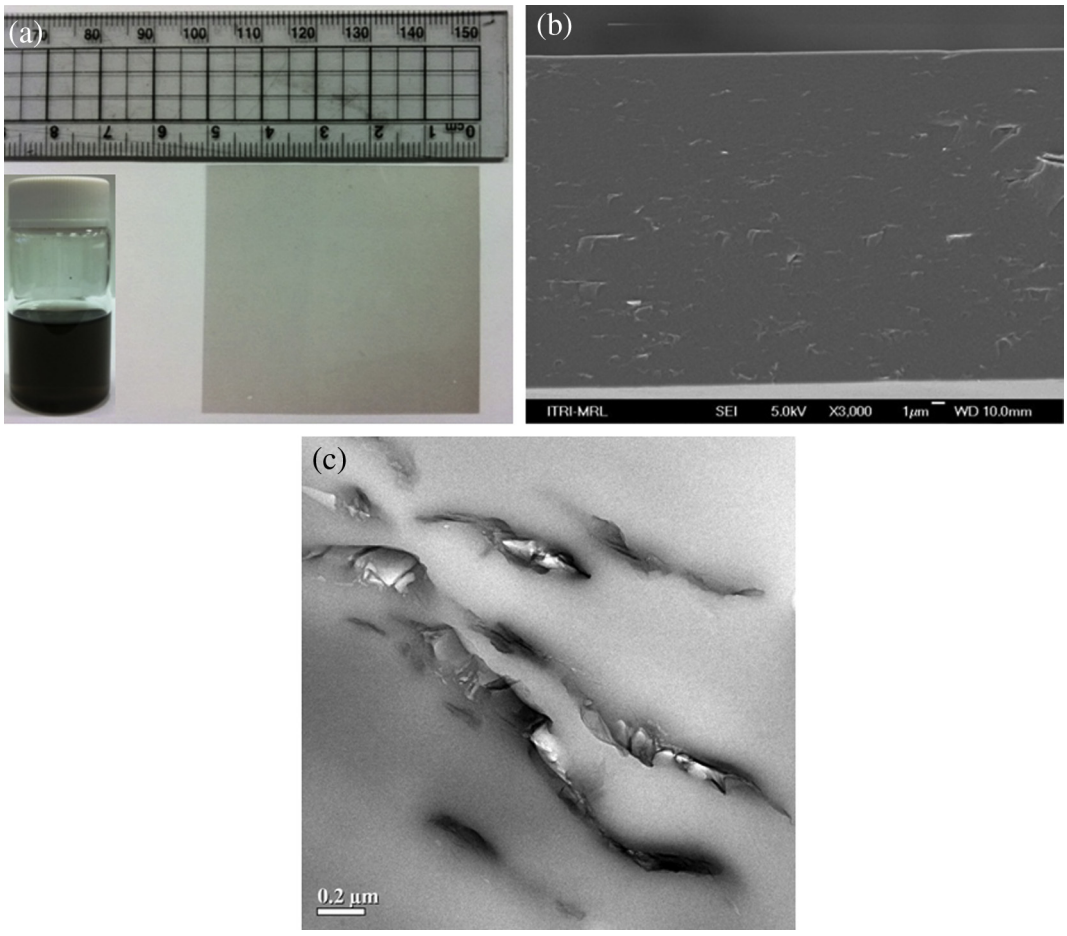

Fig. 4 – (a) Optical image of a freestanding SGO (0.05 wt%)/Nafion film (the inset shows a solution of the mixture before casting). (b) SEM and (c) TEM images provide close-up views of the microscopic morphology of the cross section.

cylindrical, or planar), and it is well accepted that the d-spacing determined by the position of the ionomeric peak represents the separation distance between hydrophilic and hydrophobic domains. The exact position of the ionomeric peak as well as a better understanding of the effect of SGO on the morphology of the Nafion matrix has shown in Fig. 6. The Nafion SAXS spectrum revealed a clear ionomeric peak because of the existence of a self-organized ionic cluster network. The position of the SAXS peak was related to the intercluster distance according to the two-phase model, or to the short-range order distance according to the core–shell model. The q value of Nafion was located at 0.6 nm^{-1}, which was lower than those for the low-weight percentage SGO/Nafion composite membranes. The Bragg spacing (d), which is

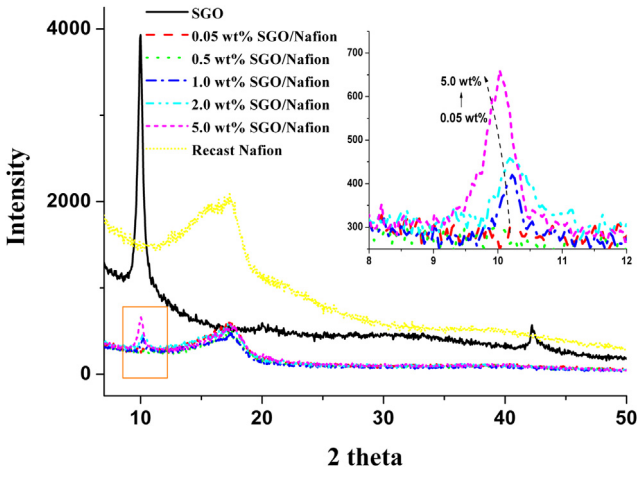

Fig. 5 – PXRD of membranes with different SGO loading percentages.

Table 1 – Water and methanol uptakes of the composite membranes.

Membrane	Water uptake	20 vol% MeOH uptake	50 vol% MeOH uptake
Nafion 115	18.4%	25.1%	48.0%
Nafion 117	18.7%	24.1%	43.1%
Recast Nafion	30.1%	36.0%	57.8%
0.05 wt% SGO	25.1%	29.1%	45.1%
0.5 wt% SGO	24.2%	27.1%	31.2%
1 wt% SGO	24.7%	28.0%	42.2%
2 wt% SGO	28.1%	28.9%	43.5%
5 wt% SGO	26.4%	27.8%	40.0%

Table 2 – Swelling ratios of the composite membranes in the presence of 20% and 50% (v/v) methanol.

Membrane	Swelling ratio (20 vol% MeOH)	Swelling ratio (50 vol% MeOH)
Nafion 115	18.4%	24.0%
Nafion 117	15.0%	23.0%
Recast Nafion	25.4%	96.0%
0.05 wt% SGO	21.0%	74.2%
0.5 wt% SGO	14.5%	32.2%
1 wt% SGO	16.6%	34.6%
2 wt% SGO	18.8%	48.8%
5 wt% SGO	16.6%	48.8%

ascribed to the average dimension of the ionic cluster, was calculated from the following equations: $d = 2\pi\, q^{-1}$ and $q = 4\pi (\lambda \sin\theta)^{-1}$. The incorporation of proper amount of SGO into the Nafion matrix decreased the d-spacing, reflecting the shrinkage of the ionic clusters which was in line with the water and methanol uptake results.

3.6. *Ionic exchange capacity (IEC) and methanol selectivity*

The incorporation of non-proton-conductive materials such as TiO_2, SiO_2, CNT, etc., into the Nafion matrix would lower its proton conductivity; thus, we used sulfonated GO (SGO) to obtain high proton conductivity. Recast Nafion with a measured IEC value of 0.962 mmeq g^{-1} was used for this study. The composite membranes showed identical IEC values due to the low ratio addition of SGO. Fig. 7 shows the relationship between the changes in proton conductivity and the SGO content, at different RH at 30 °C. Composite membranes with lower SGO content had higher proton conductivities than the recast Nafion membrane. It should be noted that the proton conductivity of Nafion at low RH was significantly decreased due to the dehydration of the ionic clusters; hence, the ability to retain absorbed water molecules could not be sustained, resulting in shrinkage of the hydrated ionic clusters. Water

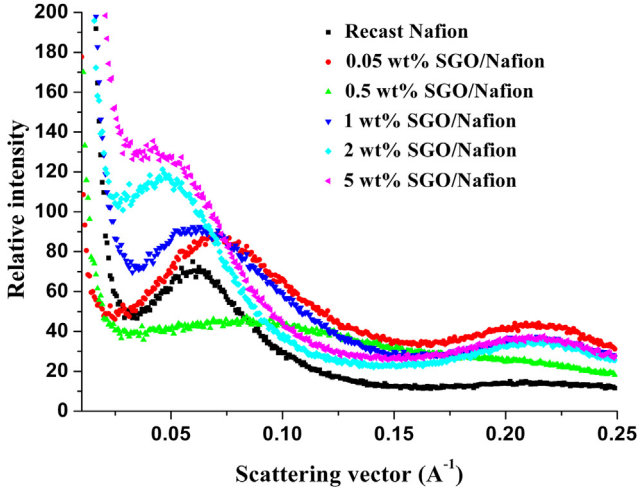

Fig. 6 – SAXS spectra of recast Nafion and SGO composite membranes.

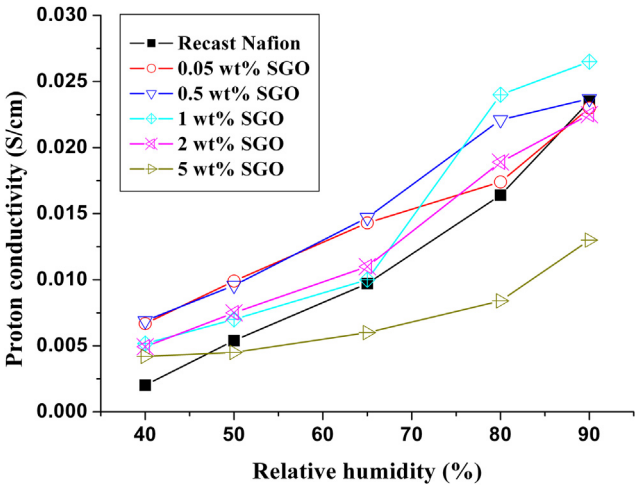

Fig. 7 – Proton conductivity of SGO composite membranes as a function of relative humidity.

retention at low humidity was obviously improved by introducing SGO into the Nafion matrix. For a low SGO content (≤0.5 wt%), the proton conductivity increased with increasing amounts of SGO, as the SGO was distributed throughout the matrix and created more interconnected transfer channels. However, with still further SGO loading, 'aggregation' began to predominate, thus reducing the conductivity of the composite membrane. For all the composite membranes, it can be seen that the proton conductivity obviously improved at low RH, indicating that the protons diffused through the hydrogen bond network of water molecules instead of a vehicle mechanism in the composite membranes as hydronium ions.

Methanol permeability is an important consideration in DMFC applications, since the crossover leads to lower cell voltages and reduced fuel efficiency. The methanol permeabilities of the composite membranes, recast Nafion membrane and commercial Nafion membranes are shown in Table 3. The methanol permeability decreased in the presence of SGO. Recast Nafion membrane exhibited a methanol permeability of 1.32×10^{-6} cm^2 s^{-1} at 30 °C, whereas the methanol permeability of 0.05 wt% SGO was 8.84×10^{-8} cm^2 s^{-1}, more

Table 3 – Proton conductivities, methanol permeabilities, and selectivities of the composite membranes, recast Nafion membrane and commercially available Nafion 115 and Nafion 117.

Membrane	Proton conductivity σ (S cm^{-1})	Methanol permeability P ($\times 10^{-6}$ cm^2 s^{-1})	Selectivity $\Phi \times 10^5$ (S cm^{-3} s)
Nafion 115	0.0399	0.447	0.89
Nafion 117	0.0412	0.435	0.94
Recast Nafion	0.0360	1.32	0.27
0.05 wt% SGO	0.0363	0.0884	4.11
0.5 wt% SGO	0.0367	0.0916	4.01
1 wt% SGO	0.0358	0.136	2.63
2 wt% SGO	0.0329	0.214	1.54
5 wt% SGO	0.0307	0.434	0.70

than a 10-fold decrease by comparison. Moreover, the SGO composite membrane had lower methanol permeability than commercial Nafion 115 and 117. Methanol transport strongly depends on the nature of water transport in the Nafion matrix. However, it was clear that the incorporation of well-dispersed SGO reduced methanol permeability because it could block the methanol from migrating through the membrane. The unique selectivity of graphene oxide was described by the A. K. Geim group [32]. GO thin films were impermeable to all gases and liquids except water. In this study, the unique high selectivity was attributed to the micron-sized and surface-modified graphene oxide.

3.7. DMA analysis of the membranes

The introduction of SGO to the Nafion matrix afforded significant mechanical reinforcement, as evidenced by the DMA traces shown in Fig. 8. Compared to pristine Nafion, the storage modulus of the 0.5 wt% SGO/Nafion membrane was higher by a factor of 1.93 at 40 °C. Substantial mechanical enhancements have been previously reported for various types of Nafion-based hybrids, including systems based on silica, carbon nanotubes, clays, and graphite oxide [33–36]. In fuel cell applications, stiffer ion-conductive materials allow the use of thinner membranes with reduced internal resistance, without the risk of structural failure. Moreover, rigid membranes can reduce dimensional changes during the assembly of the catalyst layers via hot pressing and ensure the quality of the MEA in mass production. At the same time, the tan δ curves (Fig. 8(b)) indicated that the introduction of SGO particles caused obvious displacement of the high temperature α-relaxation. The α-Relaxation has been assigned to the onset of long-range mobility of the polymeric chains (both backbone and side chains), resulting in the gradual collapse of the static network [37]. The well-dispersed SGO/Nafion composite membranes exhibited 20 °C higher tan δ than the pristine Nafion membrane, which contributed to the large interface between the exfoliated SGO and Nafion matrix.

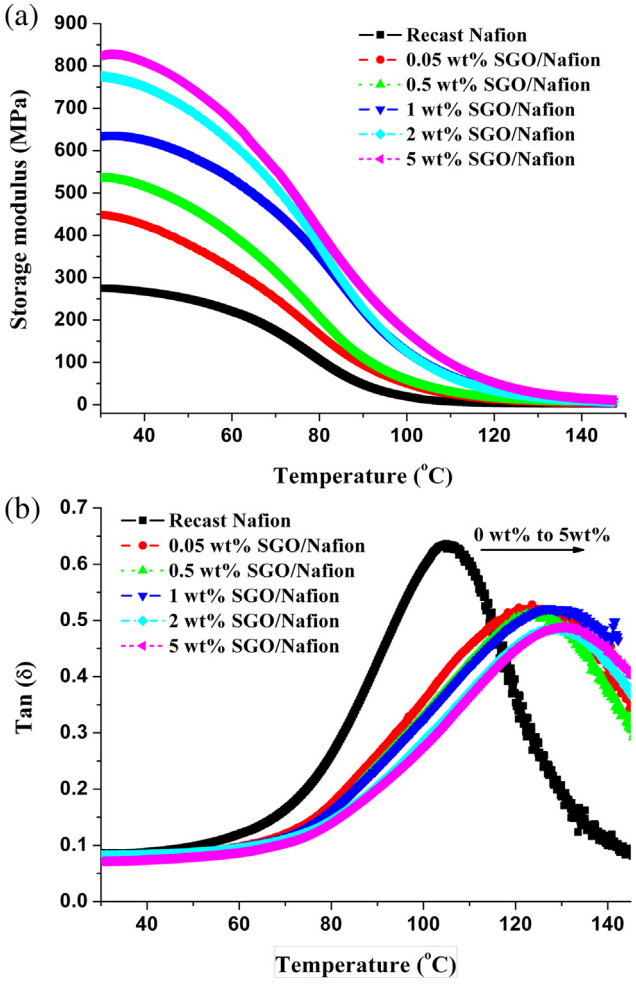

Fig. 8 – DMA traces of SGO/Nafion composite membranes: (a) storage modulus and (b) tan δ.

3.8. Performance of the DMFC

The actual cell voltages of the DMFCs are lower than the theoretical voltages due to losses involved in fuel cell operation. Major losses are due to methanol crossover from the anode to the cathode. We devised a simple method to mitigate methanol crossover by introducing SGO into the Nafion membrane. Discharge curves for the commercial Nafion 115 membrane and the composite membrane (0.05 wt%) in 1 M

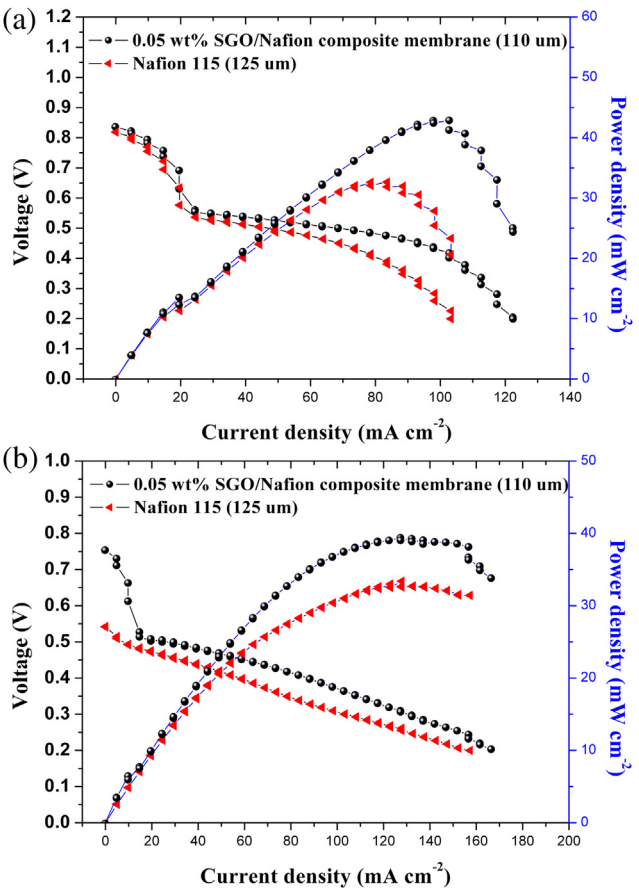

Fig. 9 – Polarization curves of DMFCs with SGO/Nafion composite membrane and Nafion membrane in (a) 1 M and (b) 5 M methanol solution.

and 5 M methanol solutions (which, here, refer to fuel) are shown in Fig. 9. The SGO/Nafion composite membrane exhibited higher current and power densities than commercial Nafion 115 under both test conditions. In 1 M methanol solution, the current density and power density for the composite membrane at 0.4 V were 102.7 mA cm^{-2} and 42.9 mW cm^{-2}, whereas the commercial Nafion 115 revealed only 78.6 mA cm^{-2} and 32.6 mW cm^{-2}. In 5 M methanol solution, the composite membrane showed values of 83.2 mA cm^{-2} (at 0.4 V) and 34.6 mW cm^{-2}, which were better than the commercial membrane (54.1 mA cm^{-2} (at 0.4 V) and 22.1 mW cm^{-2}). Additionally, the SGO/Nafion composite membrane had a slower catalyst activation loss than Nafion 115, which indicated that the composite membrane had lower methanol crossover and faster reaction kinetics. The improved performance showed good consistency with the methanol selectivity. The composite membrane demonstrated great potential for reducing methanol crossover at high methanol concentrations.

4. Conclusions

In conclusion, a low methanol-crossover SGO/Nafion composite membrane was developed by simply blending well-exfoliated $SGO_{(aq)}$ and Nafion. The optimal dispersion concentration was assessed with rheology and PXRD, which conclusively showed that the best ratio of SGO/Nafion was in the range of 0.05–0.5 wt%. The unique SGO particles were microsized in the X–Y plane and nanometers in thickness, which provided the composite membrane with extremely high selectivity by offering steric hindrance and causing shrinkage of the ionic clusters. The higher proton conductivity at low relative humidity was contributed to better water retention of the abundantly functionalized graphene oxide. The reductions in the methanol uptake and the swelling ratio in methanol consistently revealed that the composite membranes were methanol disfavor. In the DMFCs test, the SGO/Nafion composite membrane exhibited performance superior to the commercial membrane Nafion 115 in 1 M and 5 M methanol solutions. SGO is a promising material for reducing methanol crossover and shows great potential for commercial applications.

REFERENCES

[1] Steele BCH, Heinzel A. Materials for fuel-cell technologies. Nature 2001;414:345–52.
[2] Ahmed M, Dincer I. A review on methanol crossover in direct methanol fuel cells: challenges and achievements. Int J Energy Res 2011;35:1213–28.
[3] Neburchilov V, Martin J, Wang H, Zhang J. A review of polymer electrolyte membranes for direct methanol fuel cells. J Power Sources 2007;169:221–38.
[4] Ball SC. Electrochemistry of proton conducting membrane fuel cells. Platinum Met Rev 2005;49:27–32.
[5] Ling J, Savadogo O. Comparison of methanol crossover among four types of Nafion membranes. J Electrochem Soc 2004;151:A1604–10.
[6] Lin C, Wang CY. Development of high-power electrodes for a liquid-feed direct methanol fuel cell. J Power Sources 2003;113:145–50.
[7] Jiang RC, Kunz HR, Fenton JM. Composite silica/Nafion® membranes prepared by tetraethylorthosilicate sol–gel reaction and solution casting for direct methanol fuel cells. J Membr Sci 2006;272:116–24.
[8] Dimitrova P, Friedrich KA, Stimming U, Vogt B. Modified Nafion®-based membranes for use in direct methanol fuel cells. Solid State Ionics 2002;150:115–22.
[9] Rodriguez JIG, Ladewig B, Dicks A, Duke M, Costa JCDd: Proceedings of the ARCCFN Annual Conference, Coffs Harbour 2004, December 2–3. p. 10–13.
[10] Vaivars G, Maxakato NW, Mokrani T, Petrik L, Klavins J, Gericke G, et al. Zirconium phosphate based inorganic direct methanol fuel cell. Mater Sci 2004;10:162–5.
[11] Tripathi BP, Shahi VK. Recent progress on organic–inorganic nanocomposite polymer electrolyte membranes for fuel cell applications. Prog Polym Sci 2011;36:238–68.
[12] Tricoli V, Nannetti F. Zeolite–Nafion composites as ion conducting membrane materials. Electrochim Acta 2003;48:2625–33.
[13] Lin H, Zhao C, Ma W, Li H, Na H. Layer-by-layer self-assembly of in situ polymerized polypyrrole on sulfonated poly(arylene ether ketone) membrane with extremely low methanol crossover. Int J Hydrogen Energy 2009;34:9795–801.
[14] Lin CW, Fan KC, Thangamuthu R. Preparation and characterization of high selectivity organic–inorganic hybrid-laminated Nafion 115 membranes for DMFC. J Membr Sci 2006;278:437–46.
[15] Kim YM, Park KW, Choi JH, Park IS, Sung YE. A Pd-impregnated nanocomposite nafion membrane for use in high-concentration methanol fuel in DMFC. Electrochem Commun 2004;5:571–4.
[16] Tsai LD, Chien HC, Liao YH. US patent 20120172416A1.
[17] Geim AK, Novoselov KS. The rise of graphene. Nat Mater 2007;6:183–91.
[18] Park S, Ruoff RS. Chemical methods for the production of graphenes. Nat Nanotechnol 2009;4:217–24.
[19] Tung VC, Huang JH, Tevis I, Chu CW, Stupp SI, Kim F, et al. Surfactant-free water-processable photoconductive all-carbon composite. J Am Chem Soc 2011;133:4940–7.
[20] Chen S, Zhu J, Wu X, Han Q, Wang X. Graphene oxide–MnO_2 nanocomposites for supercapacitors. ACS Nano 2011;4:2822–30.
[21] Choi BG, Huh YS, Park YC, Jung DH, Hong WH, Park H. Enhanced transport properties in polymer electrolyte composite membranes with graphene oxide sheets. Carbon 2012;50:5395–402.
[22] Jiang Z, Zhao X, Fu Y, Manthiram A. Composite membranes based on sulfonated poly(ether ether ketone) and SDBS-adsorbed graphene oxide for direct methanol fuel cells. J Mater Chem 2012;22:24862–9.
[23] Hummers WS, Offeman JRE. Preparation of graphitic oxide. J Am Chem Soc 1958;80:1339.
[24] Chien HC, Tsai LD, Kelarakis A, Lai CM, Lin JN, Fang J, et al. Highly hydrated Nafion/activated carbon hybrids. Polymer 2012;53:4927–30.
[25] Huang YJ, Ye YS, Syu YJ, Huang BJ, Chang FC. Synthesis and characterization of sulfonated polytriazole-clay proton exchange membrane by in situ polymerization and click reaction for direct methanol fuel cells. J Power Sources 2012;208:144–52.
[26] Tung VC, Cote L, Kim J, Huang J. Sticky interconnect for solution-processed tandem solar cells. J Am Chem Soc 2011;133:9262–5.
[27] Guo B, Tay SW, Liu Z, Hong L. Assimilation of highly porous sulfonated carbon nanospheres into Nafion matrix as proton and water reservoirs. Int J Hydrogen Energy 2012;37:14482–91.

[28] Gierke TD, Munn GE, Wilson FCJ. The morphology in nafion perfluorinated membrane products, as determined by wide- and small-angle x-ray studies. J Polym Sci Polym Phys 1981;19:1687–704.
[29] Mauritz KA, Moore RB. State of understanding of nafion. Chem Rev 2004;104:4535–85.
[30] Williams CE, Russel TP, Jerome R, Horrion J. Ionic aggregation in model ionomers. Macromolecules 1986;19:2877–84.
[31] Roche EJ, Pineri M, Duplessix R, Levelut AM. Small-angle scattering studies of nafion membranes. Polym Sci Polym Phys Ed 1981;19:1–11.
[32] Nair RR, Wu HA, Jayaram PN, Grigorieva1 IV, Geim AK. Unimpeded permeation of water through helium-leak-tight graphene-based membrane. Science 2012;335:442–4.
[33] Cele N, Ray SS. Recent progress on Nafion-based nanocomposite membrane for fuel cell application. Macromol Mater Eng 2009;294:719–38.
[34] Burgaz E, Lian H, Alonso RH, Estevez L, Kelarakis A, Giannelis EP. Nafion-clay hybrids with a network structure. Polymer 2009;50:2384–92.
[35] Alonso RH, Estevez L, Lian H, Kelarakis A, Giannelis EP. Nafion-clay nanocomposite membranes: morphology and properties. Polymer 2009;50:2402–10.
[36] Thomassin JM, Koller J, Caldarella G, Germain A, Jerome R, Detrembleur CJ. Beneficial effect of carbon nanotubes on the performances of Nafion membranes in fuel cell applications. J Membr Sci 2007;303:252–7.
[37] Page KA, Cable KM, Moore RB. Molecular origins of the thermal transitions and dynamic mechanical relaxations in perfluorosulfonate ionomers. Macromolecules 2005;38:6472–84.